



# Potential of field hyperspectral imaging as a non destructive method to assess leaf nitrogen content in Wheat

Nathalie Vigneau<sup>a</sup>, Martin Ecartot<sup>b</sup>, Gilles Rabatel<sup>a</sup>, Pierre Roumet<sup>b,\*</sup>,

<sup>a</sup>*Cemagref, UMR ITAP, 361 rue Jean-François Breton, F-34196 Montpellier, France.*

<sup>b</sup>*INRA, UMR DIA-PC, Domaine de Melgueil, F-34130 Mauguio, France.*

---

## Abstract

Nitrogen is the most important crop limiting factor, thus plant nitrogen status during plant cycle is a key parameter for crop monitoring. Many new techniques, based on leaf optical properties have been proposed for a non-destructive diagnosis to replace Nitrogen Nutrition Index which is a costly and destructive method. We intend here to study leaf nitrogen concentration accessibility from reflectance (400-1000 nm) spectra of whole plants from a field hyperspectral imaging set-up including difficulties related to variable solar lighting and potential specular reflexion. Firstly, we calibrated a chemometrical model between leaf nitrogen concentration and reflectance spectra of flat leaves ( $R^2=0.903$ , SEP=0.327 %DM), which validated the sensor and our reflectance correction process. As a second step, we calibrated a chemometrical model between nitrogen concentration and reflectance spectra of individual leaves from isolated plants grown in pots in greenhouse ( $R^2=0.889$ , SEP=0.481 %DM) or under field conditions ( $R^2=0.881$ , SEP=0.366 %DM).

---

\*Corresponding author

*Email address:* [roumet@supagro.inra.fr](mailto:roumet@supagro.inra.fr) (Pierre Roumet)

Pooling the two datasets provided us a relevant model to predict leaf nitrogen content for the two culture conditions ( $R^2=0.875$ ,  $SEP=0.496$  %DM) suggesting that this technique is promising to assess nitrogen plant parameters with a non destructive method. This tool could be used to follow-up plant nitrogen dynamics criteria or to generate nitrogen spatial cartographies.

*Keywords:* hyperspectral, reflectance, nitrogen concentration, durum wheat

---

## 1. Introduction

As nitrogen availability in soil affects both yield and harvest quality in most annual cultivated species, nitrogen (N) is considered as key plant nutrient. During vegetative growth soil N is taken up by roots and assimilated in leaves to synthesize proteins, which are integrated in structural components to constitute cell wall or enzymes in metabolic pathways. In leaves, main part of nitrogen is involved in photosynthetic process through the Rubisco (which represents about 50 % of leaf nitrogen content, Evans (1983)) or enzymes implied in transportation or assimilation of fixed carbon.

As soil N supply is often limited, nitrogen fertilizer management should be adjusted to crop N requirements to optimize plant production (Lemaire et al., 2008). To evaluate this plant demand, a well established diagnostic tool is the Nitrogen Nutrition Index (NNI) (Lemaire and Gastal, 1997). NNI is based on comparing actual crop bulk N concentration with an empirical N dilution curve. The biomass dependent, critical N concentration ( $N_c$ ) is the minimal N concentration required for maximal growth, developed by Lemaire

18 and Salette (1984) and then adapted for most cultivated plants (Justes et al.  
19 (1994) for winter wheat, Sheehy et al. (1998) for rice, Colnenne et al. (1998)  
20 for rape, Bélanger et al. (2001) for potato and Ziadi et al. (2010) for spring  
21 wheat). Obviously the method is laborious and destructive. In other hand, as  
22 a strong relationship exists between leaf nitrogen content and photosynthetic  
23 pathway, N leaf indirect estimations based on chlorophyll measurement have  
24 been suggested (Baret and Fourty, 1997). Indirect and non destructive N  
25 methods derived from chlorophyll measurement through leaf transmittance  
26 were proposed; such as Chlorophyll meter SPAD 502®<sup>®</sup>, which provides leaf  
27 chlorophyll content based on leaf transmittance at two wavelengths : 650  
28 and 940 nm.

29

30 If some authors, as Lee et al. (1999) found a good relationship ( $R^2$  between  
31 0.81 and 0.96 according to the stages of growth) between the chlorophyll  
32 content and the actual nitrogen concentration (%DM), others works demon-  
33 strated that this linear relationship nitrogen/chlorophyll does not work in  
34 every condition; it could vary according to environmental conditions or/and  
35 cultivars (Spaner et al., 2005). To stabilize this relationship the use of ratio  
36 between data from experimental plots with overfertilizer reference plot have  
37 been recommended (Ziadi et al., 2008) although this reference plot may be  
38 sometimes difficult to put in place as underlined by Fox et al. (2001). Any-  
39 way, Houlès et al. (2007) connect successfully chlorophyll and NNI with a  
40 linear equation ( $R^2$  between 0.63 and 0.71 according to growing stage) and  
41 Ziadi et al. (2008) measured a determination coefficient of 0.61 between NNI  
42 and SPAD values. An integrated approach consists in calculating the NNI

43 using remote sensing: the biomass is found through the LAI and the nitrogen  
44 content through the chlorophyll content at the canopy scale (Houlès et al.,  
45 2007; Lemaire et al., 2008; Chen et al., 2010; Fitzgerald et al., 2010).

46

47 In these approaches, the chlorophyll-nitrogen relationship quality is the  
48 key point of the nitrogen prediction quality. Yet, this chlorophyll-nitrogen  
49 relationship depends on growing season (Evans, 1983) or on nitrogen content  
50 range as shown by Evans (1983) and Hidema et al. (1991) at leaf level.

51

52 An alternative approach was proposed by Kokaly (2001); it consists to  
53 estimate directly plant nitrogen content from a greater wavelength number  
54 from visible and infrared spectra as it was classically done in spectroscopy.  
55 Wavelength range characteristics and chemometrical models have been in-  
56 vestigated to carry out the more efficient models to predict N plant concen-  
57 tration.

58

59 Hansen and Schjoerring (2003) demonstrated that visible and NIR spec-  
60 tra from 400 to 900 nm coupled with a Partial least Square regression (PLS)  
61 allows to calibrate N plant content with  $R^2$  of 0.71 and an error of prediction  
62 of 0.38 % of dry matter, improving of 24 % nitrogen concentration prediction  
63 based on vegetation indices as the NDVI for example. Similar results were  
64 reported by Alchanatis and Schmilovitch (2005) from spectra of leaves in the  
65 field measured from 530 to 1100 nm ( $R^2 = 0.81$  and an error of prediction  
66 of 0.27 %DM) and by Morón et al. (2007) with spectra (400-2500 nm) col-  
67 lected spectra from excised fresh material ( $R^2 = 0.89$ , with prediction errors

68 of 0.64). In this later work, authors pointed out that a robust model could  
69 be obtained on fresh material, if appropriate sampling data set representing  
70 a large range of environmental conditions and different cultivars was used.

71

72 These results suggested that an alternative approach based on an ex-  
73 tended number of wavelength coupled with chemometrics could provide direct  
74 estimation of nitrogen leaf content. By diversifying calibration samples (cul-  
75 ture conditions, genotypes, etc.), the variability of the relation chlorophyll-  
76 nitrogen should be included in the model.

77 For this purpose, we built a close-range hyperspectral imaging set-up to take  
78 images above wheat plots. In this context, hyperspectral imagery combines  
79 several advantages: first, it brings a sufficient spectral resolution for a direct  
80 access to nitrogen content, as discussed above. Second, its spatial resolution  
81 allows collecting the spectra of individual leaves when observing a whole plot.  
82 Since nitrogen content of the well illuminated leaves at the top of the canopy  
83 is well correlated to the crop NNI (Farrugia, 2004), the measurement of their  
84 individual spectra enables to access NNI in a non-destructive way. Moreover,  
85 spatial nitrogen distribution makes it possible to analyse individual plants  
86 within crops; this provides an innovative tool to quantify heterogeneity in-  
87 side canopy, in context of monogenetic cultivars as well as multigenotypic or  
88 multispecific crops.

89

90 The hyperspectral imagery also presents several advantages compared  
91 with punctual spectrometers (such as SPAD 502®). First, it gives spectra  
92 of each visible leaf of the plot in one image, which is considerably time

93 saving. Furthermore, these spectra are available for each pixel of the leaf  
94 surface, providing a better representativeness of the leaf spectral information,  
95 compared to a single spectrometric measurement.

96 In counterpart, such a close-range imaging system presents some specific  
97 difficulties related to the management of variable solar lighting, specular  
98 reflection and variable illumination level due to leaf inclination. In this pa-  
99 per, we describe successive correction procedures to obtain light-independent  
100 reflectance spectra from the original images. Then the calibration of chemo-  
101 metrics models between N content and reflectance spectra for isolated wheat  
102 plants in various conditions (field and greenhouse) are presented and dis-  
103 cussed.

## 104 **2. Material and methods**

### 105 *2.1. Hyperspectral image acquisition system*

106 All hyperspectral images were acquired with a pushbroom CCD camera  
107 (HySpex VNIR 1600-160, Norsk Elektro Optikk, Norway) fitted on a tractor-  
108 mounted motorised rail (see Figure 1). The camera spectral range was from  
109 400 nm to 1000 nm divided in 160 bands (3.7 nm spectral resolution). The  
110 first image spatial dimension was determined by the 1600 across-track pixels  
111 of the CCD matrix and the second one came from the camera forward move-  
112 ment on the ramp. At 1 m above the vegetation and with a nadir sighting,  
113 the ground track was about 30 cm and the spatial resolution across track  
114 was 0.2 mm (the lens and the view angle are fixed). The spatial resolution  
115 along track was set to 0.5 mm. The integration time, i.e. the time duration  
116 during which sensor is storing light energy, was fixed manually by the user

117 depending on meteorological conditions (cloudy or sunny weather). Images  
118 were then corrected in radiance using sensor characteristics (e.g. spectral  
119 sensitivity, etc.) provided by the manufacturer.

120

## 121 *2.2. Reflectance correction*

122 As a first approximation (i.e. if we consider Lambertian surfaces), radi-  
123 ance  $L(\lambda)$  is the product of the target reflectance  $R(\lambda)$ , which is intrinsic  
124 information and the illumination during image acquisition, i.e. in our case  
125 solar lighting  $E(\lambda)$ .

126

$$L(\lambda) = R(\lambda) \cdot E(\lambda) \quad (1)$$

127 Radiance can not be used directly because illumination depends on date  
128 and meteorological conditions. To obtain the variable of interest  $R$ , it is  
129 thus necessary to know the illumination. For that purpose, spectralon®  
130 (Labsphere, Inc., New Hampshire, USA) placed in the field of view of the  
131 sensor is commonly used because it is a perfect Lambertian diffuser. Another  
132 alternative is to use a reference whose spectral characteristics are known.  
133 Indeed, in given lighting conditions:

$$L_{target} = R_{target} \cdot E \quad (2)$$

$$L_{ref} = R_{ref} \cdot E \quad (3)$$

$$R_{target} = \frac{L_{target}}{L_{ref}} \cdot R_{ref} \quad (4)$$

134 where  $R$  designs the reflectance,  $L$  the radiance, and  $ref$  the reference.  
135 In this study, we used a ceramic plate appropriate for an every day field use.  
136  $R_{ref}$  was obtained from laboratory measurements.

137 An example of raw, radiance and reflectance spectra is presented in Figure  
138 2.

139 Only reflectance spectra are used for model calibration.

140  
141 This process is theoretically correct for flat leaves but not for inclined  
142 leaves. Indeed, the leaf inclination toward the sun implies two phenomena  
143 which must be taken into account. Due to their dissimilar orientation toward  
144 the sun, all leaves do not receive the same level of illumination. They do not  
145 receive either the same level than the reference ceramic. Each illumination  
146 level is linked to the cosine of the angle between the surface and the light  
147 incidence. Because this difference is independent of the wavelength, it can  
148 be introduced as a multiplicative factor. So  $E_{leaf}(\lambda) = k_1 E_{ref}(\lambda)$  with  $E_{leaf}$   
149 is the lighting received by an inclined leaf and  $E_{ref}$ , the lighting received  
150 by the horizontal ceramic plate.

151  
152 Moreover, the Lambertian approximation above is not exact. Leaves can  
153 undergo specular reflexion, i.e. a fraction  $k$  of the incident light is reflected by  
154 the leaf with no spectral modification (Grant, 1987; Bousquet et al., 2005;  
155 Chelle, 2006). Because this specular reflexion is independent of the wave-  
156 length (Bousquet et al., 2005), we can write:

$$R_{leaf}(\lambda) = \rho(\lambda) + k \quad (5)$$

$$L_{leaf} = (\rho(\lambda) + k) \cdot k_1 E_{ref} \quad (6)$$

157 where  $\rho(\lambda)$  is the Lambertian part of the leaf reflectance and  $k$  is the  
158 specular part.

Therefore applying the correction process (equation 4) leads to :

$$\frac{L_{leaf}}{L_{ref}} \cdot R_{ref} = \frac{(\rho(\lambda) + k) \cdot k_1 E}{E}$$
$$R_{app} = k_1 \cdot \rho(\lambda) + k_2 \quad (7)$$

159 where  $R_{app}$  is the reflectance obtained after the correction process,  $\rho(\lambda)$   
160 is the Lambertian part of the leaf reflectance and  $k_1$  and  $k_2$  are two scalar  
161 factors independent of the wavelength.

162

163 As a summary, the solar lighting and the leaf inclination imply a multi-  
164 plicative effect and an additive effect on the obtained reflectance with our  
165 correction process.

### 166 2.3. Chemometrical model calibration

167 We calibrated chemometrical models between reflectance spectra (400-  
168 1000 nm) and nitrogen concentration values of individual leaves using Par-  
169 tial Least Square regression (PLS) (Martens and Næs, 1998; Wold et al.,  
170 2001). Each dataset, if the number allowed it, was split in a calibration set

171 (2/3 of the samples) and a test set (the last third) with the same distribu-  
172 tion of nitrogen concentration. We calibrated the model by cross-validation  
173 leave-one-out on the calibration set. The best calibration equation and the  
174 number of latent variables (LV) were selected on the basis of a large coefficient  
175 of multiple determination ( $R^2$ ) and a low standard error of cross-validation  
176 (SECV). SECV is the root mean square error between the actual and pre-  
177 dicted values calculated over all cross-validation calibrations. The model was  
178 then tested on the test set and its quality was evaluated with the standard  
179 error of prediction corrected of the bias ( $SEP_c$ ) calculated as following:

$$SEP_c = \sqrt{\frac{\sum(\hat{y}_i - y_i - bias)^2}{N}} \quad (8)$$

180 where  $N$  is the number of sampling of test set,  $y_i$ , the actual value of the  
181 sampling  $i$  and  $\hat{y}_i$  the predicted value for the sampling  $i$ . The bias is the  
182 mean value of the difference between actual and predicted values (this value  
183 can thus be negative). It represents the distance between the prediction and  
184 the first bisector. In the following, we will present for each model the  $SEP_c$   
185 and the bias separately.

186

187 In order to overcome leaf inclination and specular reflectance effects, we  
188 used common preprocessings. Against additive effects, we used data center-  
189 ing as recommended by Vandeginste et al. (1998). Against multiplicative  
190 effects, we used normalisation as recommended by Martens and Næs (1998).

191 The calibration and test steps were done using Matlab® software (The-  
192 MathWorks, Natick, MA, USA) and our own Matlab functions.

193 *2.4. Datasets*

194 In a first step, we have focused our attention on flat leaves in order to  
195 study potentiality of our sensor and our correction process. Cut flat leaves  
196 measurements were similar to laboratory measurements and we wanted to  
197 see if we could obtain similar results as those reported previously. In a  
198 second step, architecture effects have been taken into account. We saw in  
199 section 2.2 that leaf inclination induced illumination level differences and  
200 potential specular reflection. We studied whether it was still possible to  
201 calibrate a chemometrical model to predict nitrogen when recorded signal  
202 was modified by these phenomena.

203 *2.4.1. Flat leaves*

204 Flag leaves of about 30 various French durum wheat registered varieties  
205 were cut during the 2009 growing season between flowering and maturity.  
206 They were dried and conserved in a cold room. Leaves were put on a flat black  
207 background (we used the leaf-clip disc of a field spectrometer (FieldSpec®,  
208 Analytical Spectral Devices, Inc. (ASD), Boulder, Colorado, USA)). The  
209 reference ceramic plate was put beside leaves and the leaves were imaged  
210 with the set-up described above. On Figure 3, we can see an image obtained  
211 with this protocol.

212 Once images corrected in reflectance (with the process described in para-  
213 graph 2.2), regions of interest were drawn on the leaves to calculate a mean  
214 reflectance spectrum for each leaf. The corresponding leaf part was send  
215 to laboratory for destructive nitrogen concentration measurement (Perkin-  
216 Elmer elemental analyser (PE 2400 CHN, CNRS Cefe Montpellier)). No  
217 pre-processing was applied on this dataset because leaves were flat-imaged

218 (no specular reflexion, no illumination level issue).

#### 219 *2.4.2. Isolated plants*

##### 220 *Greenhouse plants*

221

222 During winter 2009-2010, several wheat plants were grown in pots in  
223 greenhouse with two nitrogen treatments: with or without nitrogen supply.  
224 Four French durum wheat registered varieties (Neodur, Primadur, Ixos et  
225 Lloyd) were imaged at five phenological stages (tillering, 2 nodes, flowering,  
226 450 day-degrees after flowering and maturity). For each plant, the two-upper  
227 leaves were marked with coloured plastic collars to be located on the images.  
228 After each image (Figure 4), the leaves were cut and send to laboratory for  
229 destructive nitrogen measurement. After image correction, regions of interest  
230 were drawn on the images to calculate a mean reflectance spectrum for each  
231 leaf. In order to take into account illumination level and specular reflexion,  
232 two preprocessings were applied on the dataset: normalisation and centering  
233 combined in the SNV function.

234

##### 235 *Field plants*

236

237 During the 2010 growing season, wheat field plants were imaged. In  
238 order to have isolated plants (to avoid environment effects like multiple re-  
239 flections) plants were singled by hand. On each plot, 4 leaves were marked  
240 with coloured plastic collars and all the no-marked leaves were cut (see Fig-  
241 ure 5). This protocol was repeated 5 times (on the 10<sup>th</sup>, 20<sup>th</sup> and 28<sup>th</sup> of May,  
242 the 4<sup>th</sup> of June and the 1<sup>st</sup> of July 2010 which correspond to flowering, 165

243 day-degrees after flowering, 260 day-degrees after flowering, 407 day-degrees  
244 after flowering and maturity). Once again, the SNV function was used as  
245 preprocessing.

### 246 **3. Results**

#### 247 *3.1. Nitrogen concentration range*

248 On table 1 are summarised the results of laboratory experiments for each  
249 dataset.

250 According to the experiments, leaf nitrogen concentration (LNC) varies  
251 from 0.4 %DM to 5.88 %DM. Reference LNC values have a quite continuous  
252 distribution for the flat leaf dataset and a distribution more segmented (in 2  
253 or 3 clusters) for the two other datasets.

#### 254 *3.2. Models calibrated on various datasets*

255 The model on flat leaves (called flat leaf model or  $M_f$  in the following)  
256 was calibrated without preprocessing. The best model was obtained with 5  
257 LV (Figure 6).

258 The optimal processed model on greenhouse plants (called greenhouse  
259 model or  $M_g$  in the following) required the function SNV (data normalisation  
260 and centering) and was calibrated with 6 LV (Figure 7).

261 Data normalisation and centering (SNV function) were also needed to  
262 perform the best calibration on field dataset with 4LV (called field model or  
263  $M_c$  in the following)(Figure 8).

264 For each of these three models, high  $R^2$  ( $> 0.8$ ) mean that PLS is rele-  
265 vant to extract nitrogen information from reflectance spectra. All the mod-  
266 els have a negligible bias, which show the prediction accuracy. Calibration

267 step for each model shows that LNC can be predicted with a rather low  
268 SECV ( $\leq 0.45$  %DM). Moreover, the test step (only for flat leaf model and  
269 greenhouse leaf model), using new data does not increase so much the error  
270 ( $\leq 0.48$  %DM), meaning that there is no overfitting in the model.

### 271 3.3. Cross-application of models

272 Each model calibrated on isolated plants was applied on the other and  
273 vice versa. As the field dataset nitrogen concentration range was only 0-  
274 4 %DM, the field model was applied only on the greenhouse dataset whose  
275 nitrogen concentration was inside this range (Figure 9).

276 All the data of isolated plants (greenhouse and field plants) were used  
277 to calibrate a model. The best model (called isolated plant model or  $M_t$  in  
278 the following) required once again the function SNV (data normalisation and  
279 centering) and called for only 6 LV (Figure 10).

280 Figure 11 shows the PLS-coefficients of model calibrated on isolated  
281 plants (greenhouse and field plant datasets together). The coefficient values  
282 reveal the importance of each wavelength to build the model. The most im-  
283 portant coefficients (in absolute value) correspond to chlorophyll absorption  
284 bands (660 nm) but also to other spectral bands: around 500 nm, 550 nm,  
285 700 nm, 750 nm and 930 nm.

## 286 4. Discussion

287 The objective of our work was to evaluate hyperspectral imaging as a non  
288 destructive technology to assess leaf nitrogen content in wheat leaves. In this  
289 work we used a sensor with a spectral range from 400 to 1000 nm. Our mea-  
290 sure leans so mainly on the photosynthetic nitrogen: chlorophyll, chlorophyll

291 a-proteins complexes at 675 nm (Hopkins, 2003) and some proteins accessible  
292 via their  $N - H$  bound near 900 nm (Curran, 1989). As the sun was used as  
293 light source, correction in reflectance was firstly carried out and next models  
294 was calibrated based on PLS approach. To illustrate the potential of the  
295 method, calibrations were built in two steps: firstly on dried excised leaves  
296 to specify the capacity of this technology to assess LNC and secondly on  
297 whole plant to take into account different leaf angles and variable leaf water  
298 content in the model. On excised dried flat leaves, a good accurate model was  
299 performed (Figure 6). Statistical parameters of this prediction were pretty  
300 good: the  $R^2$  - which measures the accuracy of regression - was closed to 1  
301 (0.903), the prediction error did not exceed 16% of the mean of the dataset,  
302 and bias was negligible. These results are similar to those obtained by Morón  
303 et al. (2007) ( $R^2=0.88$  and  $SECV=0.27$ ). Obviously they demonstrate the  
304 relevance of our sensor and validate our reflectance correction process to infer  
305 leaf nitrogen concentration with a good relevance.

306

307 In a second step, LNC was inferred from leaf spectra collected on fresh and  
308 non excised leaves from greenhouse or field plants. In both cases, calibrations  
309 obtained have a good accuracy:  $R^2$  values remain high ( $> 0.889$ ), prediction  
310 errors do not exceed 15% of the mean of the dataset and, as previously, the  
311 bias was negligible (Figures 7 and 8). These results are slight higher than  
312 those obtained previously by Morón et al. (2007) ( $R^2=0.82$  and  $SECV=0.74$   
313 in laboratory with a spectrometer equipped with an internal light). The  
314 combination of reflectance correction process and pre-processings (data nor-  
315 malisation and centering) was very efficient to take into account different

316 leaf inclinations on plants and possible specular reflection: our calibration  
317 quality decreases slightly but remains very relevant. These results suggest  
318 strongly that it possible to assess leaf nitrogen concentration directly from  
319 fresh leaves during plant cycle following a non destructive approach.

320

321 Although all these different models provide accurate leaf nitrogen predic-  
322 tion, these models were built on different bases. Therefore, a model built  
323 on a given dataset was not relevant to the next one: for example calibration  
324 on fresh field leaves could not be used on greenhouse leaves: the prediction  
325 bias is too high (Figure 9(a)) indicating that in our case models are dataset  
326 dependent. Both low sample number and growing conditions (especially  
327 plant nitrogen supply) could explain these differences. Correlations between  
328 leaf characteristics (physical properties as thickness, biochemical composi-  
329 tion such as chlorophyll, protein content, etc.) and LNC may vary from one  
330 experiment to the other and affect the relative importance of the different  
331 wavelengths involved in the PLS process. Otherwise, as we underlined it in  
332 introduction, the relation between photosynthetic nitrogen and total nitro-  
333 gen could vary according to environmental conditions, leaf age, etc. Anyway,  
334 pooling the two datasets (plants in greenhouse and in field) let us to propose  
335 a common model (Figure 10). The high  $R^2$  (0.875), the low SEPc and the  
336 negligible bias mean that variable growing conditions of the samples do not  
337 prevent from accessing to nitrogen information. The model coefficients of  
338 the plant model Mt (Figure 11) show that many spectral bands are solicited  
339 and not only chlorophyll absorption bands. We can thus think that using  
340 the whole spectra allow us to include chlorophyll-nitrogen relation variability

341 inside the PLS model. Indeed, Hansen and Schjoerring (2003) showed that  
342 using PLS improved the prediction (by 24 %) of the nitrogen concentration  
343 with regard to the use of vegetation indices as the NDVI for example. The  
344 results obtained by combining all the datasets suggest that including a larger  
345 dataset would allow to obtain a satisfactory robustness, provided every possi-  
346 ble situation is represented in the samples. For that it is necessary to include  
347 several genotypes, several growing years and different growing conditions (in  
348 greenhouse and in field) and particularly plant density.

## 349 **5. Conclusion**

350 A few main conclusions can be established from this study. First, nitrogen  
351 concentration is accessible from reflectance spectra in 400-1000 nm range not  
352 only from dried leaves but also from fresh samples scanned on whole plants.  
353 Secondly, reflectance correction process and pre-processings used allow to free  
354 oneself from solar lighting issues and plant architecture effects (illumination  
355 level and specular reflection) leading to the same quality than the models  
356 obtained with laboratory spectra. Moreover, using the whole spectra allow  
357 us to overcome variability due to growing conditions, compared to the use  
358 of only chlorophyll absorption bands. Nevertheless, a wide calibration set is  
359 necessary to calibrate models robust to growing conditions, year, etc.

360  
361 Finally, this study showed that field close range hyperspectral imaging is  
362 a promising technology for non destructive nitrogen monitoring. Its use can  
363 be enlarged to physiology or modeling issues. Applying this chemometrical  
364 model on whole plot hyperspectral images produces spatial nitrogen cartogra-

365 phies. It will be thus possible to follow-up nitrogen dynamics at each leaf  
366 level. Data can be introduced in growing models or nitrogen remobilisation  
367 models for example.

### 368 **Acknowledgements**

369 This study has been funded by the Garicc project of the Q@liméditerranée  
370 competitive cluster. We are very grateful to Frédéric Compan and Béatrice  
371 Ramora for their help for field experiments.

### 372 **References**

- 373 Alchanatis, V., Schmilovitch, Z., 2005. In-field assessment of single leaf ni-  
374 trogen status by spectral reflectance measurements. *Precision Agriculture*  
375 6, 25–39.
- 376 Baret, F., Fourty, T., 1997. Diagnosis on the Nitrogen Status in Crops. G.  
377 Lemaire (ed), Ch. Radiometric Estimates of Nitrogen Status of Leaves and  
378 Canopies, pp. 201–227.
- 379 Bélanger, G., Walsh, J., Richards, J., Milburn, P., Ziadi, N., 2001. Critical  
380 nitrogen curve and nitrogen nutrition index for potato in eastern canada.  
381 *American Journal of Potato Research* 78 (5), 355–364.
- 382 Bousquet, L., Lachérade, S., Jacquemoud, S., Moya, I., 2005. Leaf brdf mea-  
383 surements and model for specular and diffuse components differentiation.  
384 *Remote Sensing of Environment* 98 (2-3), 201–211.

- 385 Chelle, M., 2006. Could plant leaves be treated as lambertian surfaces in  
386 dense crop canopies to estimate light absorption? *Ecological Modelling*  
387 198 (1-2), 219–228.
- 388 Chen, P., Haboudane, D., Tremblay, N., Wang, J., Vigneault, P., Li, B., 2010.  
389 New spectral indicator assessing the efficiency of crop nitrogen treatment  
390 in corn and wheat. *Remote Sensing of Environment* 114 (9), 1987–1997.
- 391 Colnenne, C., Meynard, J., Reau, R., Justes, E., Merrien, A., 1998. Determi-  
392 nation of a critical nitrogen dilution curve for winter oilseed rape. *Annals*  
393 *of Botany* 81 (2), 311–317.
- 394 Curran, P. J., 1989. Remote sensing of foliar chemistry. *Remote Sensing of*  
395 *Environment* 30, 271–278.
- 396 Evans, J., 1983. Nitrogen and photosynthesis in the flag leaf of wheat  
397 (*Triticum aestivum* L.). *Plant Physiology* 72, 297–302.
- 398 Farrugia, A., Gastal, F., Scholefield, D., 2004. Assessment of nitrogen status  
399 of grassland. *Grass Forage Sci.* 59 (2004), 113-120.
- 400 Fitzgerald, G., Rodriguez, D., O’Leary, G., 2010. Measuring and predict-  
401 ing canopy nitrogen nutrition in wheat using a spectral index-the canopy  
402 chlorophyll content index (ccci). *Field Crops Research* 116 (3), 318–324.
- 403 Fox, R., Piekielek, W., Macneal, K., 2001. Comparison of late-season di-  
404 agnostic tests for predicting nitrogen status of corn. *Agronomy Journal*  
405 93 (3), 590–597.

- 406 Grant, L., 1987. Diffuse and specular characteristics of leaf reflectance. *Re-*  
407  *mote Sensing of Environment* 22 (2), 309–322.
- 408 Hansen, P., Schjoerring, J., 2003. Reflectance measurement of canopy  
409 biomass and nitrogen status in wheat crops using normalized difference  
410 vegetation indices and partial least square regression. *Remote Sensing of*  
411  *Environment* 86, 542–553.
- 412 Hidema, J., Makino, A., Mae, T., Ojima, K., 1991. Photosynthetic charac-  
413 teristics of rice leaves aged under different irradiances from full expansion  
414 through senescence. *Plant Physiology* 97, 1287–1293.
- 415 Hopkins, W. G., 2003. *Physiologie végétale*. Bruxelles : De Boeck.
- 416 Houllès, V., Guérif, M., Mary, B., 2007. Elaboration of a nitrogen nutrition  
417 indicator for winter wheat based on leaf area index and chlorophyll content  
418 for making nitrogen recommendations. *European Journal of Agronomy*  
419 27 (1), 1–11.
- 420 Justes, E., Mary, B., Meynard, J., Machet, J., Thelier-Huche, L., 1994. De-  
421 termination of a critical nitrogen dilution curve for winter wheat crops.  
422 *Annals of Botany* 74 (4), 397–407.
- 423 Kokaly, R., 2001. Investigating a physical basis for spectroscopic estimates of  
424 leaf nitrogen concentration. *Remote Sensing of Environment* 75 (2), 153–  
425 161.
- 426 Lee, W., Searcy, S., Kataoka, T., 1999. Assessing nitrogen stress in corn  
427 varieties of varying color. In: 1999 ASAE Annual International Meeting.

- 428 No. Paper No 99-3034 in ASAE Meeting Presentation. ASAE, 2950 Niles  
429 Rd., St. Joseph, MI 49085-9659 USA, Toronto, Ontario Canada.
- 430 Lemaire, G., Gastal, F., 1997. Diagnosis of the Nitrogen Satus in Crops.  
431 G. Lemaire (Ed.), Ch. N Uptake and Distribution in Plant Canopies, pp.  
432 3–43.
- 433 Lemaire, G., Jeuffroy, M.-H., Gastal, F., 2008. Diagnosis tool for plant and  
434 crop n status in vegetative stage. theory and practices for crop n manage-  
435 ment. *European Journal of Agronomy* 28 (4), 614–624.
- 436 Lemaire, G., Salette, J., 1984. Relationship between dynamics of growth and  
437 of nitrogen uptake in a pure grass stand. i. study of environmental effects.  
438 *Agronomie* 4, 423–430.
- 439 Martens, H., Næs, T., 1998. *Multivariate calibration*. John Wiley & Sons.
- 440 Morón, A., García, A., Sawchik, J., Cozzolino, D., 2007. Preliminary study on  
441 the use of near-infrared reflectance spectroscopy to assess nitrogen content  
442 of undried wheat plants. *Journal of the Science of Food and Agriculture*  
443 87 (1), 147–152.
- 444 Sheehy, J., Dionora, M., Mitchell, P., Peng, S., Cassman, K., Lemaire, G.,  
445 Williams, R., 1998. Critical nitrogen concentrations: Implications for high-  
446 yielding rice (*oryza sativa* l.) cultivars in the tropics. *Field Crops Research*  
447 59 (1), 31–41.
- 448 Spaner, D., Todd, A., Navabi, A., McKenzie, D., Goonewardene, L., 2005.  
449 Can leaf chlorophyll measures at differing growth stages be used as an in-

- 450     indicator of winter wheat and spring barley nitrogen requirements in eastern  
451     canada? *Journal of Agronomy and Crop Science* 191 (5), 393–399.
- 452     Vandeginste, B. G. M., Massart, D. L., Buydens, L. M. C., De Jong, S., Lewi,  
453     P. J., Smeyers-Verbeke, J., 1998. *Handbook of Chemometrics and Quali-*  
454     *metrics: Part B. Vol. 20B of Data Handling in Science and Technology.*  
455     Elsevier Science.
- 456     Wold, S., Sjöström, M., Eriksson, L., 2001. PLS-regression: a basic tool of  
457     chemometrics. *Chemometrics and Intelligent Laboratory Systems* 58, 109–  
458     130.
- 459     Ziadi, N., Bélanger, G., Claessens, A., Lefebvre, L., Cambouris, A., Tremblay,  
460     N., Nolin, M., Parent, L.-E., 2010. Determination of a critical nitrogen  
461     dilution curve for spring wheat. *Agronomy Journal* 102 (1), 241–250.
- 462     Ziadi, N., Brassard, M., Bélanger, G., Claessens, A., Tremblay, N., Cam-  
463     bouris, A., Nolin, M., Parent, L.-E., 2008. Chlorophyll measurements and  
464     nitrogen nutrition index for the evaluation of corn nitrogen status. *Agron-*  
465     *omy Journal* 100 (5), 1264–1273.

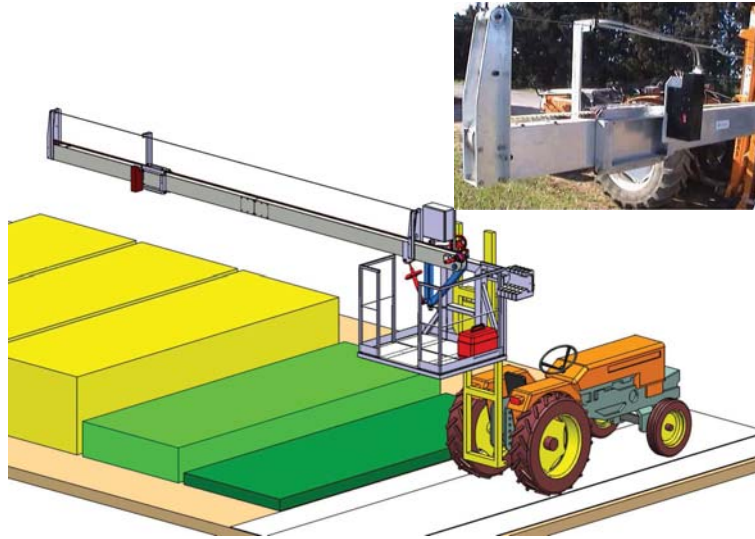
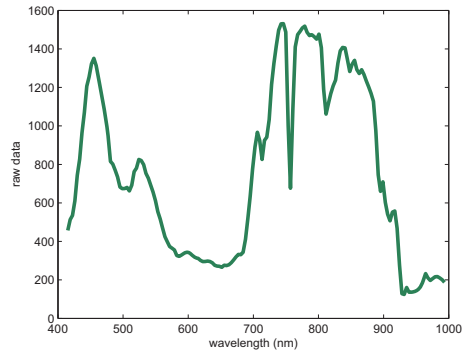


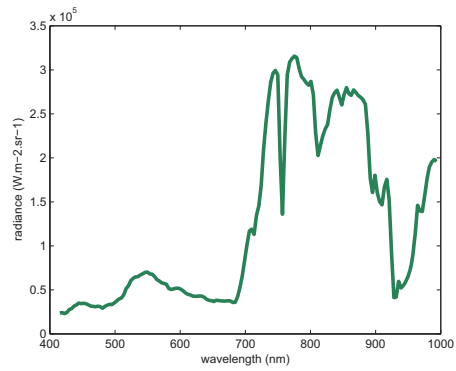
Figure 1: Hyperspectral imaging set-up.

Table 1: Nitrogen concentration range for each dataset: nitrogen concentrations are in %DM

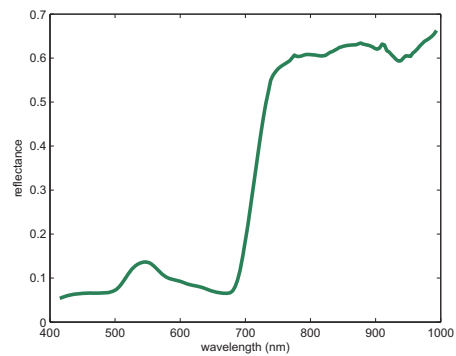
dataset	n	min	max	mean	standard deviation
flat leaves	146	0.4	3.78	2.07	1.05
greenhouse plants	180	0.81	5.88	3.22	1.42
field isolated plants	56	0.71	4.2	2.37	1.07



(a)



(b)



(c)

Figure 2: Example of (a) raw, (b) radiance and (c) reflectance spectra for an isolated leaf. Absorption peaks due to the atmosphere are removed in (c) by the reflectance correction.

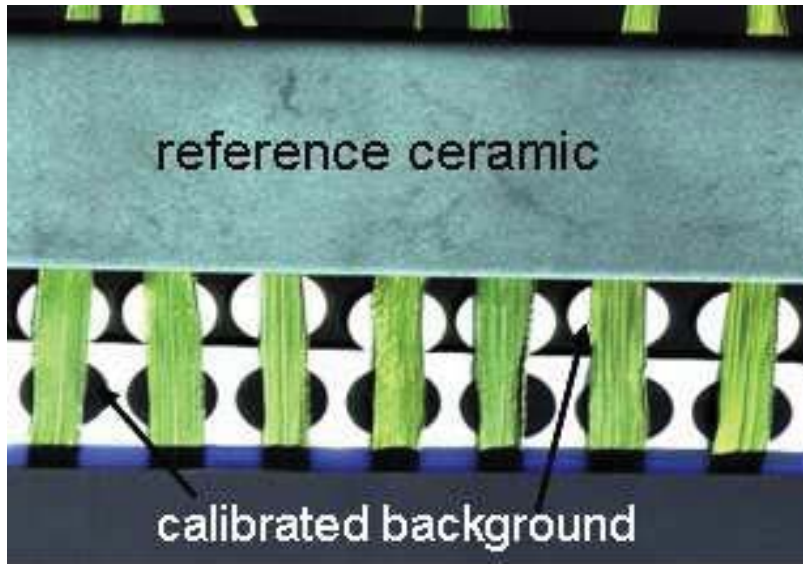
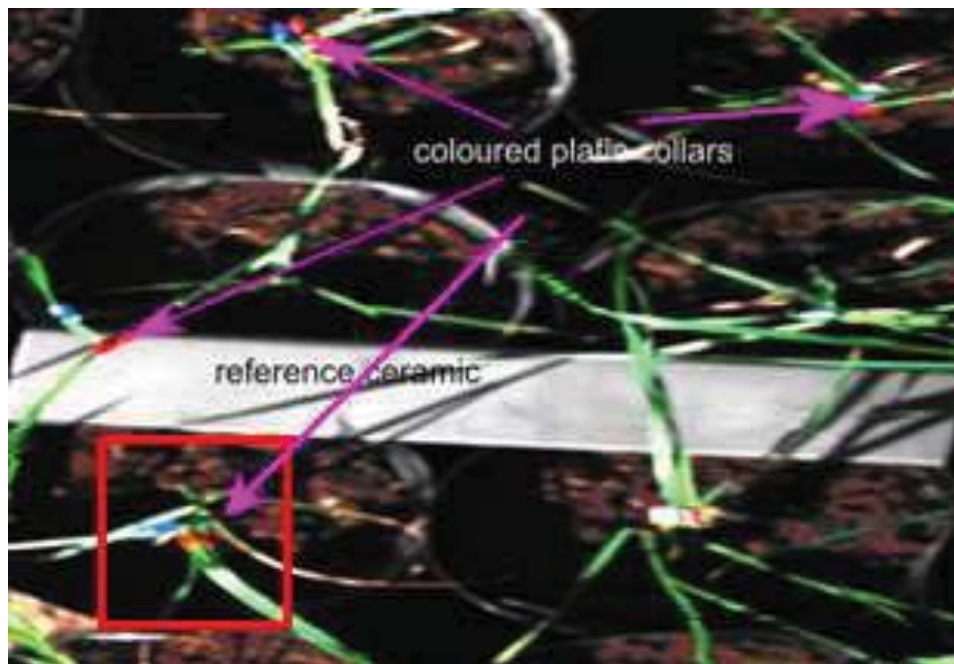
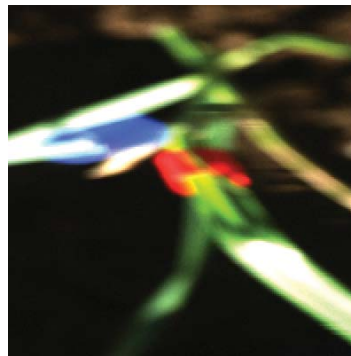


Figure 3: Example of an image obtained with the protocol for flat leaves (black and white background discs were set but only black ones are used in this study).



(a)



(b)

Figure 4: Example of an image obtained with the protocol for greenhouse plants.

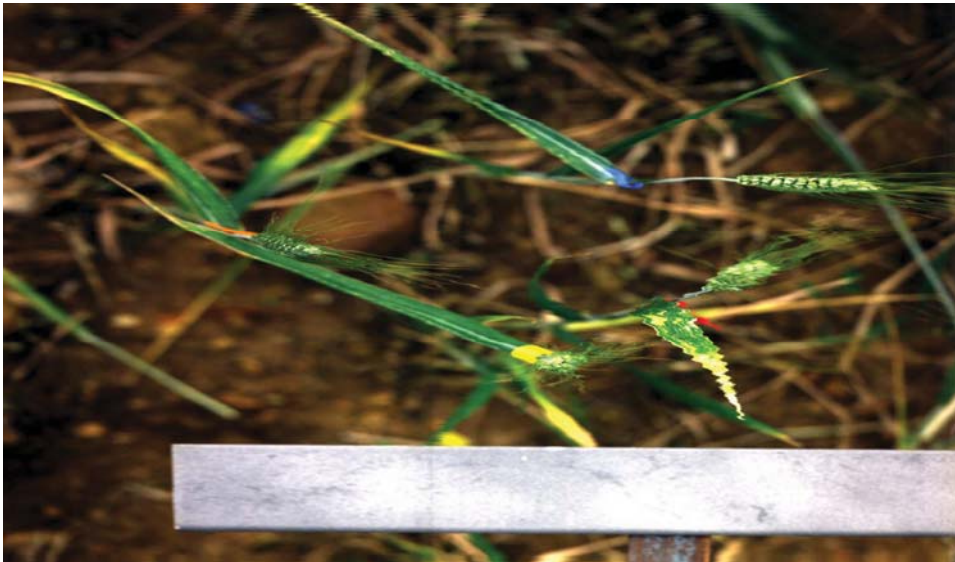


Figure 5: Example of an image obtained with the protocol for field isolated plants.

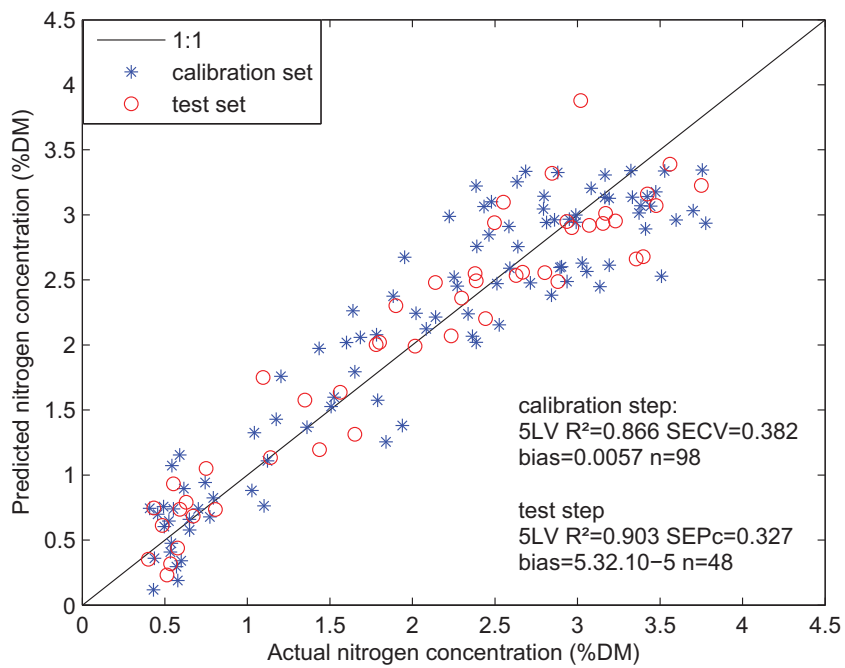


Figure 6: Results of the chemometrical model calibrated on flat leaves with no preprocessing and 5LV (blue stars for calibration step and red circles for test step).

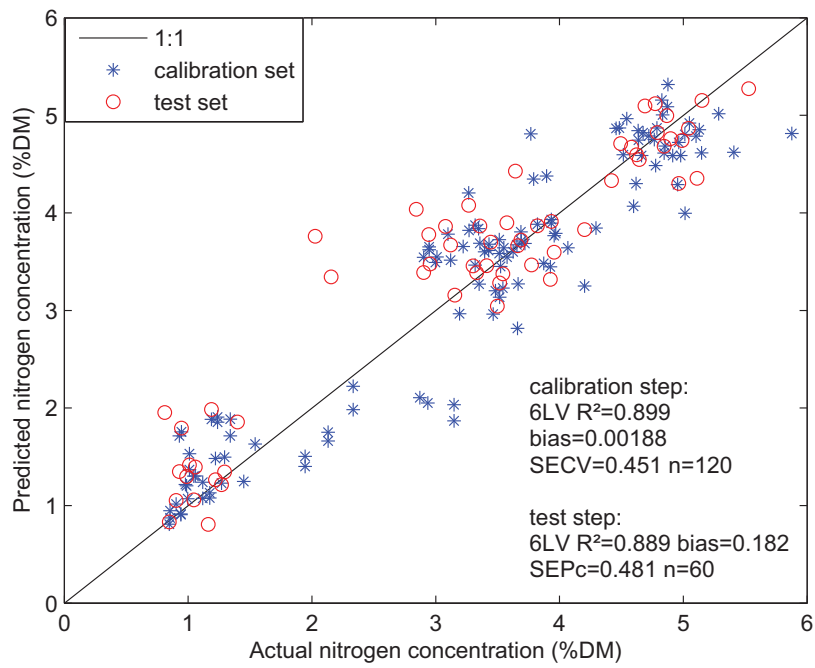


Figure 7: Results of the chemometrical model calibrated on greenhouse plants with SNV and 6LV (blue stars for calibration step and red circles for test step).

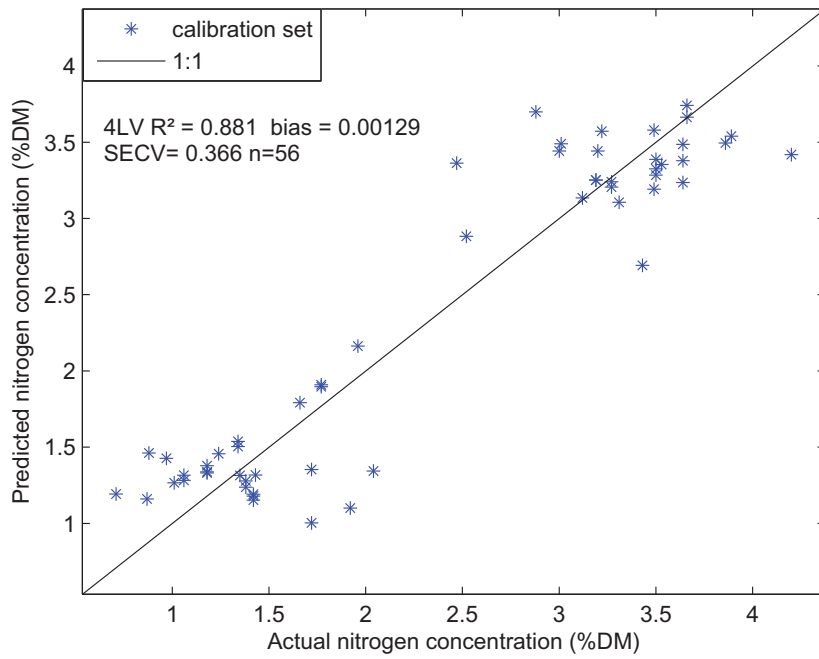
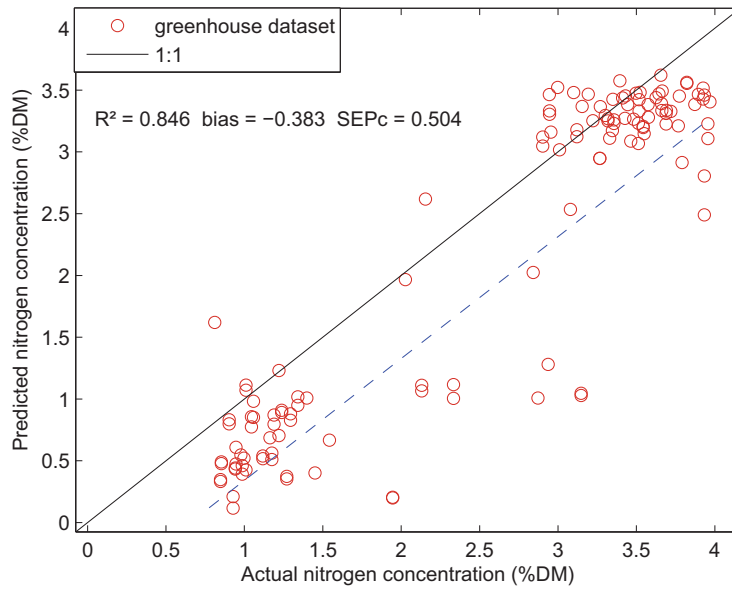
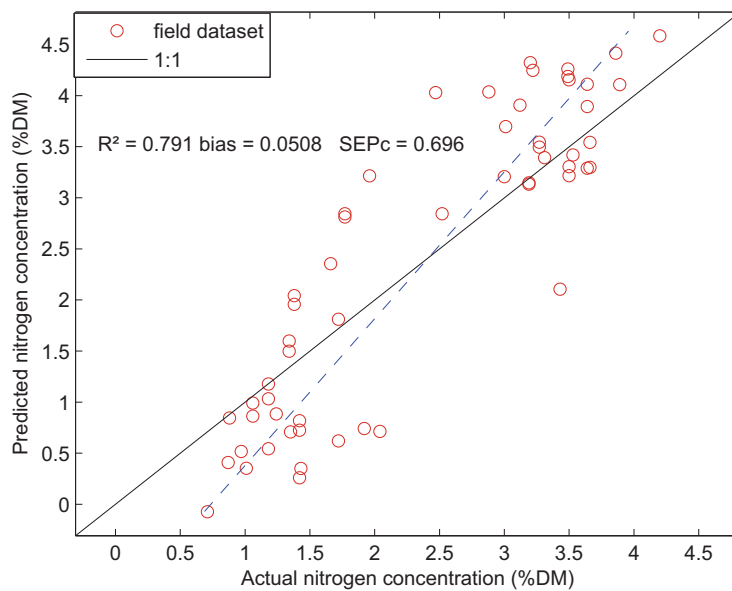


Figure 8: Results of the chemometrical model calibrated on field isolated plants with SNV and 4LV.



(a)



(b)

Figure 9: Cross-application of the models calibrated on isolated plants: (a) model calibrated on field plants applied on greenhouse plants, (b) model calibrated on greenhouse plants applied on field plants.

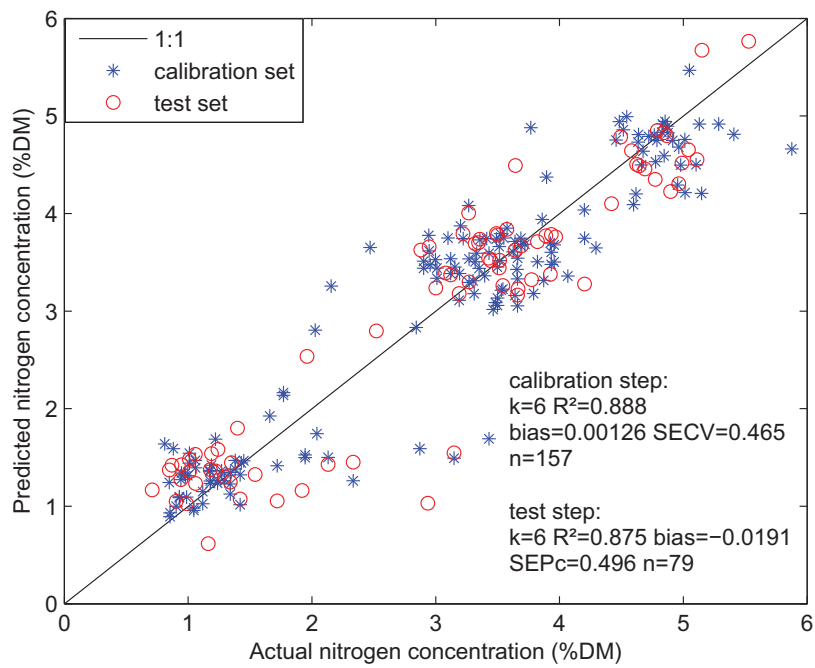


Figure 10: Results of the chemometrical model calibrated on isolated plants (greenhouse and field plants) with SNV and 6LV (blue stars for calibration step and red circles for test step).

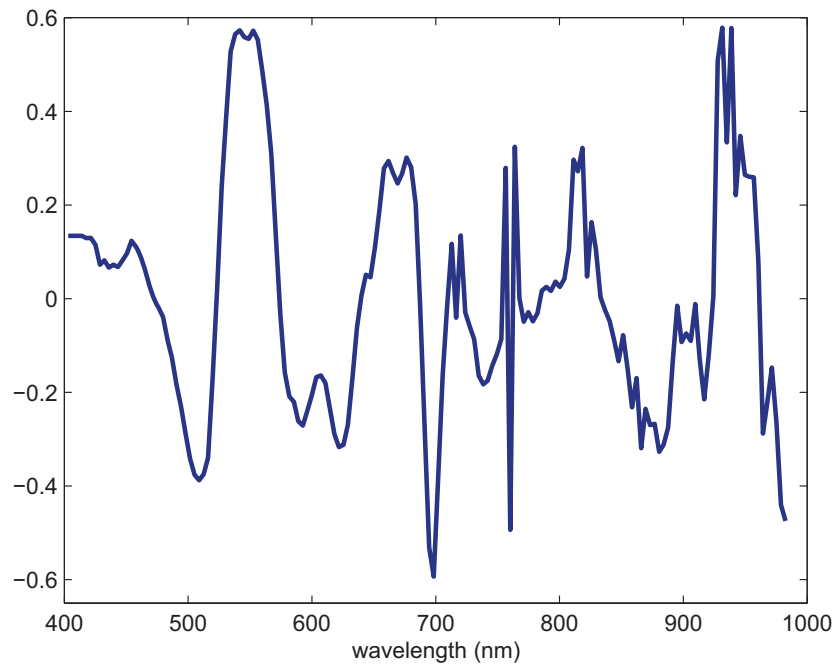


Figure 11: PLS-coefficients for the isolated plant models  $M_t$ .